Bioorganic & Medicinal Chemistry Letters 21 (2011) 3324–3328

Contents lists available at ScienceDirect

Bioorganic & Medicinal Chemistry Letters

journal homepage: www.elsevier.com/locate/bmcl

N-Hydroxy-*N*′-aminoguanidines as anti-cancer lead molecule: QSAR, synthesis and biological evaluation

Arijit Basu [a,*], Barij N. Sinha [a], Philipp Saiko [b], Geraldine Graser [b], Thomas Szekeres [b]

[a] Department of Pharmaceutical Sciences, Birla Institute of Technology, Mesra, Ranchi 835215, India
[b] Department of Medical and Chemical Laboratory Diagnostics, Medical University of Vienna, Waehringer Guertel 18-20, A-1090 Vienna, Austria

ARTICLE INFO

Article history:
Received 6 February 2011
Revised 17 March 2011
Accepted 4 April 2011
Available online 9 April 2011

Keywords:
QSAR
Pharmacophore modeling
N-Hydroxy-*N*′-aminoguanidines
N-Hydroxysemicarbazides
Ribonucleotide Reductase

ABSTRACT

The intrinsic pharmacophore model (r^2_{pred} and r^2_m of 0.858 and 0.725) has been developed and used as a query to screen in-house built library based on *N*-hydroxy-*N*′-aminoguanidine (HAG) analogs. The pharmacophoric modeled based HITs were synthesized and evaluated for anticancer activity and cytotoxicity. One of the compounds (**15**) appeared as promising lead candidate with an IC_{50} value of 11 μM yielded in HL-60 promyelocytic leukemia cells. Compound **15** reveals significantly lower cytotoxicity against HeLa and Vero cell with CC_{50} values of more than 100 μM.

Hydroxyaminoguanidines (HAGs),[1–3] hydroxamic acids,[4] hydroxysemicarbazides (HSs),[5] and amidoximes[6] were extensively explored as anticancer agents. These compounds bear similar pharmacophoric features (-C (=X) NHOH; X = O, NH), which was identified as the basic pharmacophore for anti-tumor activity.[7–9] Amongst these compounds, HAGs and HSs were explored for over three decades primarily against L1210 murine leukemia.[2,3,5] They were found to inhibit DNA synthesis as a consequence of specifically inhibiting the R2 subunit of the enzyme Ribonucleotide Reductase (RR).[10] RR is one of the most widely accepted anticancer targets[11] and considered for further exploration through computer aided design. The current work is therefore initiated primarily with the objective of building a ligand based model by exploring various pharmacophore modeling options. The method employed here consists of 3D Pharmacophore space modeling (PHASE, version 3.0, Schrödinger, LLC, New York, NY, 2008).

In the current study, 3D-QSAR strategies were explored to develop a robust QSAR model, which reveals significant external predictability. Here, we present lead design, identification, synthesis and anti-cancer evaluation based on developed QSAR model.

Structural datasets[2,3,5] (Table 1) were chosen and divided into training (75%) and test (25%) set. The compounds were clustered as per our earlier methodology[12,13] according to increasing order of biological activity. Sequentially, every fourth molecule was chosen as a test set molecule resulting to a 25% sorted test set.

Pharmacophoric sites were created using the default settings in PHASE (Schrodinger, LLC)[14] with hydrogen bond acceptor (A), hydrogen bond donor (D), hydrophobic (H), positive (P) and ring aromatic (R). A few four point hypotheses were identified, consisting of acceptor (A), one donor (D), and one ring aromatic (R) in different combinations (AAAR, ADDR and AADR). The AADR combination survived during the scoring process, their survival scores were in the range of 2.6–3.2 (Table 2a).This combination yielded six hypotheses. The best hypothesis (1) consists of four pharmacophoric features, with two acceptor (A1 and A2), one donor (D), and one ring aromatic (R) (Fig. 1 a and b). The pharmacophoric distances are shown in Table 2b. The training set comprises two types of analogs, HSs and HAGs. The average fitness for HS and HAGs were 2.74 and 2.65, respectively. The most active compound T36 (HAG analog) showed superior fitness of 2.84.

We used solely statistical metrics for model validation due to the unavailability of any co-crystal structure depicting the active site of RR. Further, it precluded the use of receptor based information and overlay study during pharmacophore-hypothesis generation for validation. Thus, a satisfactory hypothesis has been used for the development of pharmacophore based QSAR model and validated through various statistical metrics. The QSAR models were subjected for external validation employing various statistical metrics,[12,15,16] which provided significant model (r^2 = 0.989, F = 220.14, q^2 = 0.889 $r^2_{\text{Pred}} = 0.858$, $r^2_m = 0.725$, ${}^{c}R^2_p = 0.742$, Table 2a). The

* Corresponding author.
E-mail address: arijit4uin@gmail.com (A. Basu).

0960-894X/$ - see front matter © 2011 Elsevier Ltd. All rights reserved.
doi:10.1016/j.bmcl.2011.04.009

Table 1
Structures of derivatives of *N*-hydroxy-*N*′-aminoguanidine and *N*-hydroxysemicarbazide used for QSAR model building

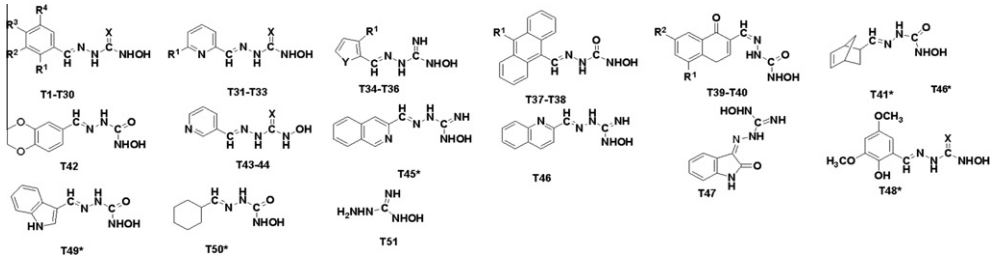

Code	R^1	R^2	R^3	R^4	X	Y	PI_{50}
T1	-OH	-Cl	-H	-Cl	O	–	5.187
T2	-OH	-H	-H	Br	O	–	4.996
T3*	-OH	-Br	-H	Br	O	–	5.143
T4	-OH	$-OCH_3$	-H	Br	O	–	4.424
T5	-H	I	-H	-H	O	–	4.095
T6	-OH	I	-H	I	O	–	5.328
T7	-H	-H	-CN	-H	O	–	3.681
T8	-H	-H	$-N(CH_3)_2$	-H	O	–	3.350
T9	-H	$-NO_2$	-H	-H	O	–	3.399
T10	-H	$-OCH_3$	-H	-H	O	–	3.433
T11	$-OCH_3$	-H	-H	$-OCH_3$	O	–	4.521
T12	-OH	-H	OCH_3	-H	O	–	4.220
T13*	-H	-H	$-OCH_2Ph$	-H	O	–	4.318
T14	-H	-H	-Ph	-H	O	–	4.370
T15	-OH	-H	-OH	-H	O	–	3.883
T16	-H	I	-H	-H	NH	–	4.902
T17	-H	$-CF_3$	-H	-H	O	–	4.403
T18*	-H	-H	$-OCH_3$	-H	O	–	3.499
T19	-H	$-CF_3$	-H	-H	NH	–	4.821
T20	-H	$-OCH_3$	-H	-H	NH	–	4.796
T21*	-H	-H	$-OSO_2CH_3$	-H	NH	–	4.830
T22	-H	NO_2	-H	-H	NH	–	5.119
T23	-H	-	-CN	-H	NH	–	5.027
T24	-OH	-Br	-H	-Br	NH	–	4.783
T25	-H	$-NO_2$	-Cl	-H	NH	–	4.896
T26	-H	-H	$-OCH_2C_6H_5$	-H	NH	–	4.597
T27	$-OCH_3$	-H	-H	$-OCH_3$	NH	–	5.149
T28	-H	-H	$-CF_3$	-H	NH	–	5.036
T29*	-H	-H	$-O(CH_2)_5CH_3$	-H	NH		5.108
T30	-H	-H	$-O(CH_2)_3CH_3$	-H	NH		5.069
T31	-H	–	–	–	NH	–	4.962
T32	$-CH_3$	–	–	–	NH	–	4.376
T33	$-CH_3$	–	–	–	O	–	3.050
T34	$-CH_3$	–	–	–	–	S	4.479
T35*	-H	–	–	–	–	S	4.467
T36	-H	–	–	–	–	NCH_3	5.569
T37*	$-CH_3$	–	–	–	–	–	5.357
T38	-Cl	–	–	–	–	–	5.268
T39	-Cl	-Cl	–	–	–	–	4.550
T40*	-H	$-C(CH_3)_2$	–	–	–	–	4.492
T41*	–	–	–	–	–	–	4.975
T42	–	–	–	–	–	–	3.749
T43	–	–	–	–	NH		4.636
T44	–	–	–	–	O		3.217
T45*	–	–	–	–	–	–	5.481
T46	–	–	–	–	–	–	5.167
T47	–	–	–	–	–	–	4.315
T48*	–	–	–	–	–	–	4.039
T49*	–	–	–	–	–	–	3.322
T50*	–	–	–	–	–	–	4.673
T51	–	–	–	–	–	–	3.900

* Test set molecules, $PI_{50} = -\log_{10}IC_{50}$

QSAR model was shown in Figure 2 which demonstrates favorable (blue) and unfavorable (red) regions.

One of the significant observations while visualizing this QSAR model was the large clustering of the blue boxes near the ring aromatic (R) feature, suggesting larger rings/multiple rings are favorable for biological activity. The scatter plot of predicted PI_{50} versus observed PI_{50} (Fig. 3a and b) confirms the superiority of the developed model. The scatter plot for the test set (Fig. 3b) indicates a reasonably good correlation ($r^2_{Pred} = 0.858$) between the predicted and experimental activities. Further, it reveals the way test and training set compounds were chosen. Both sets were constituted with compounds covering a wide range of actives, resulting in a classic 'cigar' shaped plot rather than a 'dumbbell' plot.

Table 2a
Pharmacophoric hypothesis developed for the particular data set[a]

Hyp ID	Survival	Site	Volume	Selectivity
1[b]	3.178	0.72	0.651	0.984
2	3.078	0.67	0.623	0.99
3	3.075	0.68	0.612	0.991
4	2.998	0.59	0.606	0.991
5	2.571	0.51	0.38	0.988
6	2.566	0.37	0.51	1.019

[a] No of ligand matched = 39
[b] QSAR analysis of HYP ID 1 resulted in the following statistics $r^2 = 0.989$, $F = 220.14$, $q^2 = 0.889$ $r^2_{pred} = 0.858$, $r^2_m = 0.725$, $^cR^2_p = 0.742$.

Table 2b
Inter-pharmacophoric distances for hypothesis 1

Site1	Site2	Distance
A1	A2	4.711
A1	D	3.892
A1	R	3.753
A2	D	2.023
A2	R	8.463
D	R	7.475

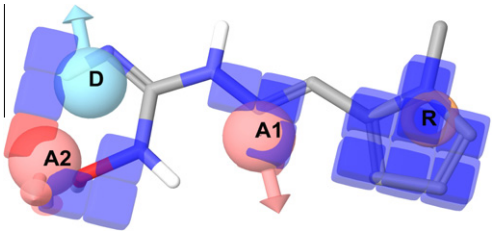

Figure 2. QSAR model visualized in the context of the most active compound **T36**. Blue regions show favorable regions, red disfavored regions.

Therefore, the obtained predictive QSAR model can be utilized as a query tool for 3D databases screening to identify possible lead as anticancer agent. An in-house library was constructed with the synthetically feasible fragments using SMILIB.[17]The constructed library was then predicted against the developed model. Eight molecules (**1**, **2**, **5**, **6**, **7**, **10**, **11**, **12**, **14**, and **15**) were identified as significant HITs for synthesis. However, five non-significant molecules (**3**, **4**, **8**, 9 and **13**) were also chosen for synthesis to evaluate the true negatives.

Synthesis[18]of compounds (**3**-**15**) were outlined in Scheme 1. Structures of the synthesized compounds are given in Table 3 physicochemical properties and spectral details are given in Supplementary data. The synthesized compounds (**3**-**15**) were screened against the HL-60 human promyelocytic leukemia cell line[19,20] and also screened for their cytotoxic potential against HeLa and Vero cell cultures. Five compounds (**6**, **10**, **11**, 14 and **15**) were found to be active against HL-60 human promyelocytic leukemia cells yielding IC_{50} values between 11–95 μM (Table 3). Compound **15** showed promise with an IC_{50} value of 11 μM and relatively high cytotoxic concentration (CC_{50}) of >100 μM (Supplementary Table). The pharmacophoric fitness (Fig. 1a) of compound **15** was 2.26. This was overall satisfactory and comparable to compounds with similar activity.

The experimental and predicted values are in congruence (Table 3). Moreover, identification of five true negatives (**3**, **4**, **8**, 9 and **13**) by the developed QSAR model is trulyoutstanding. The fitness score for these ligands were less than two; the fitness poses were shown in Fig. 1d.

These observations further consolidate the model, enabling it to be further explored for screening additional databases in future. Compound **15** with an IC_{50} of 11 μM and relatively high cytotoxic concentration >100 μM have been identified as the lead molecule.

The study was focused on exploring possible ligand based modeling options to develop robust QSAR model(s) for the particular kind of analogs. These models were validated computationally as well as experimentally. The resulting robust and reproducible

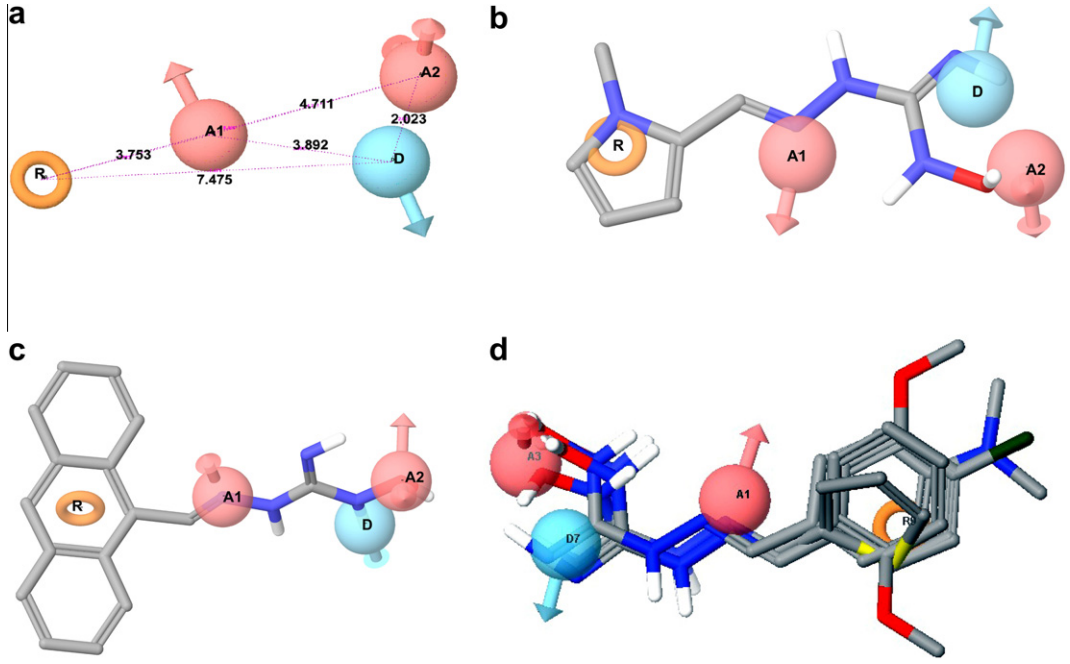

Figure 1. (a) Pharmacophore maps of the generated model. The distance between the various pharmacophoric features are given. Hydrogen bond acceptor (A), hydrogen bond donor (D), hydrophobic (H), positive (P) and ring aromatic (R). (b) Most active molecule **T36** is embedded in the map. (c) Newly synthesized compound **15** is embedded in the map. (d) Fitness of five true negatives on the developed hypothesis.

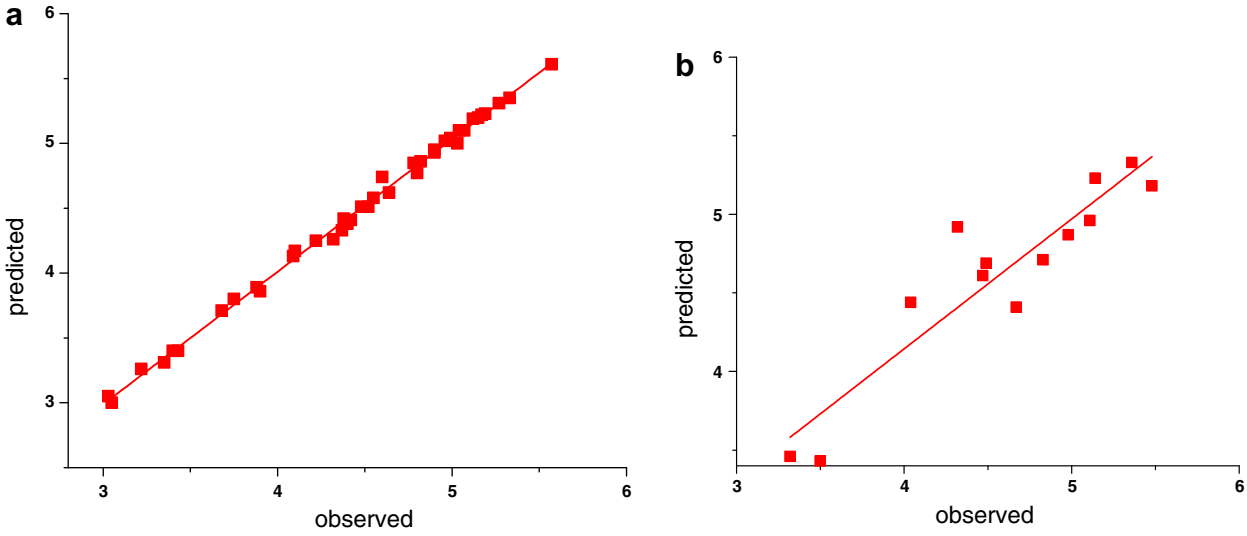

Figure 3. Red line indicates the 'best fit' amongst the predicted and experimental PI_{50}. (a) Training set compounds, (b) test set compounds.

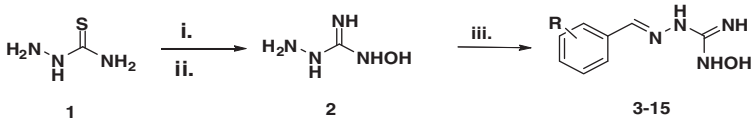

Scheme 1. Reagents and conditions: (i). CH_3I/MeOH, 12 h, rt, (ii) NH_2OH, MeOH, rt, 4 h (iii) Ar-CHO, MeOH, reflux 3 h.

QSAR model can be used as a query tool for future drug design for this particular class of compounds. We have also identified a lead molecule which is not only outstanding, but can also be a good starting point with an IC_{50} of 11 μM, CC_{50} > 100 μM i.e. a selectivity index of more than 10. Detailed biochemical studies for compound 15 were recently reported by our group.[21] It proved to be a potent inhibitor of RR and arabinofuranosylcytosine (Ara-C) synergist.

Table 3
Structure, biological activity (growth inhibition of HL-60 human promyelocytic leukemia cells) and cytotoxicity of the synthesized compounds.

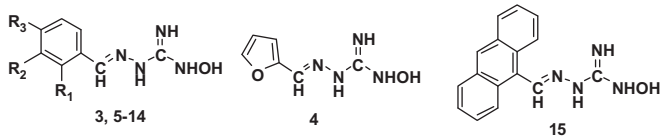

Code	R^1	R^2	R^3	HL-60 IC_{50} (μM)		CC_{50} (μM)	
				Pred	Exp	HeLa Cells	VERO Cells
3	-H	-H	$-N(CH_3)_2$	285	>100	>100	>100
4	—	—	—	156	>100	>100	>100
b	-H	-H	-OH	54	>100	>100	>100
6	-OH	-H	-H	78	95	>100	>100
7	$-OCH_3$	-H	-H	230	>100	>100	>100
8	-H	-H	$-OCH_3$	246	>100	>100	>100
9	$-CH_3$	-H	-H	156	>100	>100	>100
10	-H	-H	$-CH_3$	72	67	>100	>100
11	-Cl	-H	-H	98	60	>100	>100
12	-H	-H	-Cl	154	>100	>100	>100
13	-H	-OH	$-OCH_3$	254	>100	>100	>100
14	-H	-H	-H	56	62	>100	>100
15	—	—	—	9	11	>100	>100

IC_{50} = 50% growth inhibition of HL-60 cells, CC_{50} = 50% growth inhibition of HeLa and VERO cell line.

Due to these promising results, it deserves further preclinical and in vivo testing and might be good candidate molecule for further lead optimization.

Acknowledgments

This work was supported by University Grants Commission, India. We are thankful to Dr. Ashoke Sharon, Dr. Venkatesan J. and Nibha Mishra who has helped to improve the structure and language of our manuscript. We thank to Dr. Kunal Roy for helping us out with $^cR_p^2$ determination. Vlife Sciences, for providing the trial version of MDS and Schrodinger, LLC for helping in extraction of QSAR descriptors.

Supplementary data

Supplementary data associated with this article can be found, in the online version, at doi:10.1016/j.bmcl.2011.04.009.

References and notes

1. Koneru, P. B.; Lien, E. J.; Avramis, V. I. *Pharm. Res.* **1993**, *10*, 515.
2. Tai, A. W.; Lien, E. J.; Lai, M. M.; Khwaja, T. A. *J. Med. Chem.* **1984**, *27*, 236.
3. T'Ang, A.; Lien, E. J.; Lai, M. M. *J. Med. Chem.* **1985**, *28*, 1103.
4. van't Riet, B.; Wampler, G. L.; Elford, H. L. *J. Med. Chem.* **1979**, *22*, 589.
5. Ren, S.; Wang, R.; Komatsu, K.; Bonaz-Krause, P.; Zyrianov, Y.; McKenna, C. E.; Csipke, C.; Tokes, Z. A.; Lien, E. J. *J. Med. Chem.* **2002**, *45*, 410.
6. Fylaktakidou, K. C.; Hadjipavlou-Litina, D. J.; Litinas, K. E.; Varella, E. A.; Nicolaides, D. N. *Curr. Pharm. Des.* **2008**, *14*, 1001.
7. Nocentini, G. *Crit. Rev. Oncol. Hematol.* **1996**, *22*, 89.
8. Tsimberidou, A. M.; Alvarado, Y.; Giles, F. J. *Expert. Rev. Anticancer Ther.* **2002**, *2*, 437.
9. Cerqueira, N. M.; Pereira, S.; Fernandes, P. A.; Ramos, M. J. *Curr. Med. Chem.* **2005**, *12*, 1283.
10. Shao, J.; Zhou, B.; Zhu, L.; Bilio, A. J.; Su, L.; Yuan, Y. C.; Ren, S.; Lien, E. J.; Shih, J.; Yen, Y. *Biochem. Pharmacol.* **2005**, *69*, 627.
11. Shao, J.; Zhou, B.; Chu, B.; Yen, Y. *Curr. Cancer Drug Targets* **2006**, *6*, 409.

12. Basu, A.; Jasu, K.; Jayaprakash, V.; Mishra, N.; Ojha, P.; Bhattacharya, S. *Eur. J. Med. Chem.* **2009**, *44*, 2400.
13. Dewangan, P.; Verma, S.; Basu, A. *Lett. Drug Des. Discovery* **2008**, *5*, 494.
14. *PHASE procedure.* Six built-in types of pharmacophoric features: hydrogen bond acceptor (A), hydrogen bond donor (D), hydrophobic (H), negative ionizable (N), positive ionizable (P), and aromatic ring (R). Ligands were processed with the LigPrep program to assign protonation states appropriate for pH 7.0. Conformer generation was carried out with the MacroModel. Potentials were computed using the OPLS2005 force field. The default pharmacophore feature definitions were used in site generation. After the identification of the sites hypotheses were generated by a systematic variation of the number of sites. The number of matching active compounds was kept default of 39 (entire training set). All the molecules were considered as active no active/inactive threshold were assigned. The scoring was done using: Survival score formula = (Vector score) + (Site score) + (Volume score) + (Selectivity score) + (Number of matches-1)−(Reference ligand relative conformational energy) + (Ref ligand activity). Max intersite distance=2.00Å, initial and final box size is 20 Å and 1 Å, respectively. The best hypothesis was chosen based on the survival score by PHASE. The top scored hypothesis was then used to build pharmacophore-based 3D QSAR models with 3 PLS factors and Grid spacing = 1 Å.
15. Roy, P.; Roy, K. Q. S. A. R. *Comb. Sci.* **2008**, *27*, 302.
16. Mitra, I.; Saha, A.; Roy, K. *Molecular Simulation* **2010**, *36*, 1067.
17. Schüller, A.; Schneider, G.; Byvatov, E. Q. S. A. R. *Comb. Sci.* **2003**, *22*, 719.
18. (a) General method for synthesis of *N*-Hydroxy-*N*'-amino guanidine (2).Thiosemicarbazide (0.5 mol) and Methyl iodide (0.5 mol) in methanol (500 mL) was stirred at rt for 12 h to form *S*-methylisothiosemicarbazide. The base was liberated using equimolar amount of sodium bicarbonate. The precipitate was filtered and washed with cold water and finally with cold methanol: Yield 90%, mp 108–110 °C. $C_2H_6N_2S_2$, C, 19.71%; H, 4.95%; N, 23.02%; S, 52.59%. The resulting *S*-methylisothiosemicarbazide (0.4 mol) was reacted with hydroxylamine (0.5 mol) solution (A cold solution of potassium hydroxide (0.5 mol) in 250 mL of methanol was added to a cold hydroxyamine hydrochloride) at room temperature and stirred for 4 h. The solution was concentrated under reduced pressure on cooling crude *N*-Hydroxy-*N*′-amino guanidine separates out, which is then re-crystallized from ethanol. Yield 70%, mp 119–121 °C. CH_6N_4O, C, 13.43%; H, 6.68%; N, 62.06%.
(b)General method for synthesis of compounds (**3**–**15**). *N*-hydroxy-*N*′-amino guanidine (0.5 mol) and different aromatic aldehydes (0.5 mol) were refluxed for 3 h to obtain different compounds **3**–**15**. The resulting compounds were re-crystallized from 95% ethanol. Compound **15**: Yield 78%, mp 160 °C, FAB-MS 278(M+), 279 (M+1), ^{1}H NMR (DMSO, 400 MHz) δ 7.5–8.6 (m, 5H, $C_{14}H_9$), δ 8.67(s, 1H, CH), δ 9.25(s, 1H, NH), δ 10.52s, 1H, NH), δ 11.32 (s, 1H, OH).
19. Saiko, P.; Ozsvar-Kozma, M.; Bernhaus, A.; Jaschke, M.; Graser, G.; Lackner, A.; Grusch, M.; Horvath, Z.; Madlener, S.; Krupitza, G.; Handler, N.; Erker, T.; Jaeger, W.; Fritzer-Szekeres, M.; Szekeres, T. *Int. J. Oncol.* **2007**, *31*, 1261.
20. Madlener, S.; Illmer, C.; Horvath, Z.; Saiko, P.; Losert, A.; Herbacek, I.; Grusch, M.; Elford, H. L.; Krupitza, G.; Bernhaus, A.; Fritzer-Szekeres, M.; Szekeres, T. *Cancer Lett.* **2007**, *245*, 156.
21. Saiko, P.; Graser, G.; Giessrigl, B.; Lackner, A.; Grusch, M.; Krupitza, G.; Basu, A.; Sinha, B.; Jayaprakash, V.; Jaeger, W. *Biochem. Pharmacol.* **2011**, *81*, 50.